Research Article *Science, Engineering and Health Studies 2020, 14(1), 22-31*

Selenium nanoparticles biosynthesized by garlic extract as antimicrobial agent

Pinprapha Sribenjarat[1], Nuananong Jirakanjanakit[2] and Kalyanee Jirasripongpun[1*]

[1]*Department of Biotechnology, Faculty of Engineering and Industrial Technology, Silpakorn University, Nakhon Pathom 73000, Thailand*
[2]*Institute of Molecular Biosciences, Mahidol University, Nakhon Pathom 73170, Thailand*
[*]*Corresponding author: jirasripongpun_k@su.ac.th*

Received: October 21, 2019; Revised: February 4, 2020; Accepted: February 4, 2020

ABSTRACT

Staphylococcus aureus is an important human pathogen. Its drug resistance strains could result in hospital-acquired infections. In recent years, the use of nanoparticles has become a new approach to combat antibiotic-resistant bacterial strains. In the present study, green synthesis of selenium nanoparticles (SeNPs) was conducted using garlic (*Allium sativum*) extract (G). Formation of SeNP-G was characterized by red brick solution with maximum absorbance in the range of 270-280 nm. Particles formed at 4 h (SeNP-G4) and 72 h (SeNP-G72) of incubation were spherical in shape with size range within 21-40 nm and 41-50 nm, respectively. Zeta potential analysis of the particles was at -23.8 mV and -24.2 mV, respectively. These SeNP-G exhibited higher antibacterial activity than garlic extract in a dose-dependent manner by agar diffusion method and broth dilution assay. However, no significant difference in antibacterial capability was observed between these two particle sizes. SeNP-G72 was less cytotoxic to normal human MRC-5 cell than SeNP-G4 and sodium selenite. Thus, green nanotechnology could be used to reduce toxicity of sodium selenite and enhance antibacterial activity of garlic extract by using SeNP-G as a potential antibacterial agent against *S. aureus*.

Keywords: selenium nanoparticles; garlic; antibacterial; *Staphylococcus aureus*; cytotoxicity

1. INTRODUCTION

Staphylococcus aureus, a Gram-positive bacterium, is an important human pathogen. It is responsible for numerous infections and syndromes ranging from skin infection to severe and potentially fatal invasive diseases. Infection with this bacterium is difficult to treat due to its biofilm formation and the development of antibiotic-resistant strains, which frequently results in hospital-acquired disease (Skov and Jensen, 2009). Therefore, alternative treatments are necessary in addition to commonly utilized drugs.

Nanotechnology is the creation of extremely small particles or materials in the size range of 1-100 nm, which may adapt well to interaction with bacteria as a bactericidal agent in infected areas (Wang et al., 2006). Metallic nanoparticles are fabricated by reducing a suitable bulk material to nanosize through various physical or chemical methods. A simple and fast method in nanotechnology is applying green synthesized-metal nanoparticles using plant extracts as reducing and capping agents (Mittal et al., 2013). Fresh garlic (*Allium sativum*) extract has been reported as an effective

antibacterial agent for *S. aureus* (Ratthawongjirakul and Thongkerd, 2016). However, the inhibitory activity of this material could be gradually decreased due to decomposition of allicin over time (Fujisawa et al., 2008). Nanotechnology could then be used to solve this problem as well as enhancing antimicrobial activity of the plant extract (Fardsadegh et al., 2019). Among various metallic nanoparticles, silver nanoparticles are the most widely used for biosynthesis. However, selenium nanoparticles (SeNPs) have been attractive because of their excellent biological activities, biocompatibility, and low toxicity (Menon et al., 2018), thereby making them suitable for medical application (Hosnedlova et al., 2018). SeNPs have also been reported on bacterial inhibition and anticancer activities (Mittal et al., 2013; Nguyen et al., 2017). The antibacterial activity against *S. aureus* of SeNPs varied among several synthesis techniques. Chemically synthesized SeNPs through the reduction of sodium selenite by glutathione and stabilizing agent of bovine serum albumin provided SeNPs with size in the range of 40-100 nm (Tran and Webster, 2011). These SeNPs could inhibit *S. aureus* in non-concentration dependent at concentration range of 7.8-31 (µg/mL). By contrast, SeNPs under a similar synthetic technique showed dose-dependent antimicrobial properties against *S. aureus* as bacteriostatic activity rather than bactericidal activity (Nguyen et al., 2017). Physically synthesized by laser ablation of wavelength from ultraviolet (UV) to near infrared radiation (355, 532, and 1064 nm) provided SeNPs with particle size from 80 to 300 nm, which exhibited an inhibitory effect on *Escherichia coli* growth at the extent depending on incubation time (Guisbiers et al., 2016). Furthermore, SeNPs synthesized using free-cell supernatant of *Bacillus licheniformis* provided spherical nanoparticles at a size range of 10-50 nm, which inhibited most tested Gram-positive bacteria (*Bacillus cereus, Enterococcus faecalis,* and *S. aureus*) and Gram-negative bacteria (*E. coli, Salmonella enterica serovar Typhimurium,* and *Salmonella enterica serovar Enteritidis*) (Khiralla and El-Deeb, 2015). Biogenic SeNPs played a good role in antibacterial activity. Therefore, SeNPs were synthesized using garlic extract, and its inhibitory effect on *S. aureus* was determined.

2. MATERIALS AND METHODS

2.1 Materials

Selenious acid (H_2SeO_3), 3-[4,5-dimethylthiazol -2-yl]-2,5-diphenyl tetrazolium bromide (MTT), phosphate buffer saline were purchased from Sigma-Aldrich (USA). Eagle's minimum essential medium (MEM), trypsin EDTA, penicillin-streptomycin were purchased from Gibco (USA). Dimethyl sulfoxide (DMSO) was obtained from Amresco (USA). Fetal bovine serum was purchased from Hyclone (USA). Garlic extract powder was gifted from Khoalaor Laboratories CO., Ltd. (Thailand). *Staphylococcus aureus* (TISTR 746) was obtained from the MIRCEN Culture Collection (Thailand Institute of Scientific and Technological Research, Thailand). Human lung normal cell, MRC-5 (CCL-171) was obtained from the American Type Culture Collection.

2.2 Synthesis of SeNPs from garlic extract

For SeNP-G production, 0.06 g of garlic extract was dissolved in 20 mL of 10 mM sodium selenite (Sigma; S5261; Sigma-Aldrich, Singapore). Ascorbic acid (Chem-Supply BN: 289855) solution at 80 mM was added dropwise until the solution turned from colorless to slightly yellow. Then, the mixture was incubated on a shaker (MS Orbital Shaker, Major Science) at 130 rpm in the dark. Sediments of selenium nanoparticles from 4, 24, 48, and 72 h incubation periods were collected by centrifugation at 20,000 g (Z36 HK, Hermle) and washed twice with distilled water before being air-dried. The dried samples were suspended in water and sonicated for 2-5 min before they were used in the experiments.

2.3 Characteristics of SeNPs

The formation of SeNP-G was observed from the

change of color solution to brick orange. The collected SeNP-G sample was characterized by a UV-Vis spectrophotometer (Libra S22, Biochrom). Their sizes and shapes were briefly analyzed by scanning electron microscopy (Mira3, TESCAN), and the dried SeNP-G samples were carefully mounted on SEM stubs using adhesive tape. Scanning was performed under different magnifications ranging from ×20,000 to ×200,000 and voltage at 20 kV. Sizes of particles from various images were measured using Image J software. Zeta potential or charge distribution was analyzed using Zetasizer Nano ZS (Malvern Instruments) equipped with a laser (633 nm). Samples were diluted with Milli-Q water at ambient temperature to a final concentration of 5 mg/mL of SeNPs.

2.4 Bacterial culture

A sterile 10-loop (TISTR 746) was used to remove *S. aureus* from the frozen stock and streaked onto a nutrient agar. The streaked plate was then incubated at 37°C for 24 h. Bacteria from a single colony were collected using a sterile loop and inoculated into a test tube containing 5 mL of nutrient broth. The test tube was agitated in a shaking incubator at 37°C, 200 rpm, to achieve a bacterial solution at the exponential phase of growth or until cell concentrations of approximately 10^8 CFU/mL were reached.

2.5 Antibacterial tests

The antibacterial test on *S. aureus* was performed by agar diffusion and broth dilution methods. For the agar diffusion method, 100 µL of bacterial culture at approximately 3-5×10^6 cells was evenly swabbed on 25 mL of nutrient agar plates. After plate drying, cork borer was used to make holes on the agar. Thereafter, 30 µL of sample solutions were dropped. Mixed antibiotics of penicillin and streptomycin were used as positive control and distilled water was used as negative control. Zone of bacterial inhibition was measured after incubation at 37°C for 24 h.

For the broth dilution method, various concentrations of SeNP-G and equal volume of bacteria culture at 12×10^5 cells/mL were added onto each well of 96 well plates. Distilled water at the same volume of sample was used as negative control. The tested plate was then incubated for 24 h. The survival bacteria numbers were measured by a microplate reader (Sunrise, TECAN, Australia) with optical density at 600 nm. Growth inhibition of bacteria was determined based on the formula, and IC50 values were determined from the graph plot.

$$\%\ growth\ inhibition = \left(\frac{OD\ control - (OD\ sample - OD\ sample\ blank)}{OD\ control}\right)100$$

2.6 Cytotoxicity tests

Fibroblast cell of human lung normal tissue, MRC-5 (American Type Culture Collection, CCL-171), was used. The cells were cultured and maintained in MEM supplemented with 10% fetal bovine serum. Cells wTITere incubated in the presence of 10% CO_2/95% air at 37°C incubator and were passaged at split ratio of 1:3-1:5. For cytotoxicity assay, the cell was cultured in a 96-well plate for 24 h. The tested cells were treated with various concentrations of sodium selenite (0-20 µM) and SeNP-G (0, 3.125, 12.5, 50, and 200 (µg/mL), for 24 h. Thereafter, MTT assay was performed to determine the viability of the tested cells. The cell sheet was washed with PBS, added with MTT reagent and further incubated for 4 h. Then, the solution was removed and the formazan product was dissolved by DMSO. The absorbance was then measured using a microplate reader at a wavelength of 590 nm. The percentage of cell viability under different concentrations of SeNP-G was calculated using the following formula.

Thereafter, IC50 values were computed based on graphical analysis at the point where cell viability is at 50%.

$$\%\ cell\ viability = (\frac{OD\ of\ test\ well}{OD\ control})100$$

2.7 Statistical analysis

All experiments were performed in triplicate, and each was repeated at least three times. Significant differences were computed by one-way ANOVA and two sample T-test using IBM SPSS version 22.0.

3. RESULTS AND DISCUSSION

3.1 Biosynthesis of SeNPs using garlic extract

Addition of ascorbic acid changed in the reactant solution from colorless to light yellow, which implied fabrication initiator of ascorbic acid as reported by Ramamurthy et al. (2013). Phytomolecules of garlic extract further reduced selenite and coated selenium element, which gradually resulted in orange brick color of SeNP-G during the incubation period. This color demonstrated the formation of SeNPs as previously reported (Zhang et al., 2001; Lin and Chris Wang, 2005; Sharma et al., 2014). The sediment of particles collected at 4, 24, 48, and 72 h exhibited UV-vis spectrum as shown in Figure 1. The maximum absorbance of all samples from varying incubation times were in the range of 270-280 nm, while those collected at 4 h showed the clearest peak, similar to the findings of Anu et al. (2017) that the absorbance peak of SeNP-G was at 260 nm. Nonetheless, Vyas and Rana (2017) reported the absorbance peak at 400 nm of SeNP-G after incubating for 24 h. However, SeNP-G synthesized by Ezhuthupurakkal et al. (2017) using fresh garlic extract and 30 mM of seleneous acid revealed an absorbance peak in the range of 200-300 nm after 48 h incubation. In the present study, the maximum absorbance peak of SeNPs collected at 24 h was at 270 nm, whereas that for the SeNPs collected at 48 h and 72 h was at 280 nm. With longer curing time, the particles seemed to shift to the longer wavelength from the results observed at 400-500 nm. The percentage yield was computed from the amount of dried SeNP-G that could be formed from the given amounts of reactants, in percent. The yield of samples at 24, 48, and 72 h incubation time was higher (30.1 ± 10.7%, 31.5 ± 7.4%, and 33.7 ± 7.4%, respectively) compared with that at 4 h period (9.4 ± 3.4%). Coating of phytomolecules at longer period may affect the size of SeNP-G and its biological activity. To elucidate this hypothesis, we further characterized SeNP sediments collected at 4 h (SeNP-G4) and 72 h (SeNP-G72) on size and antibacterial activity.

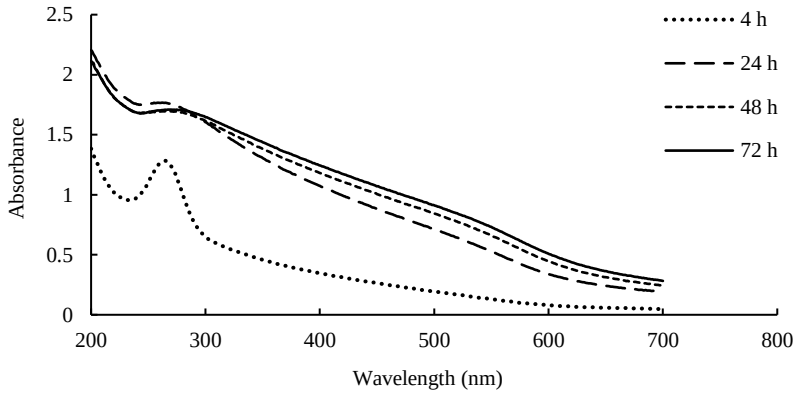

Figure 1 UV-vis absorbance spectra of garlic SeNPs solution at 4, 24, 48, and 72 h of incubation

The SEM images of SeNPs showed spherical particles (Figure 2A) with size of approximately 21-40 nm for SeNP-G4 (Figure 2B) and approximately 31-50 nm for SeNP-G72 (Figure 2D). The selenium nanoparticles at longer curing times may be coated with additional content of phytomolecules from garlic extract, resulting in slightly larger particles. This condition was in accordance with the shift of absorbance peak of SeNP-G72 to longer wavelength compared with SeNP-G4, which also implied its larger particle size, similar to the findings of Lin and Chris Wang (2005) that the extent of orange appearance and red-shift of absorption spectra was correlated with the increase of particle size.

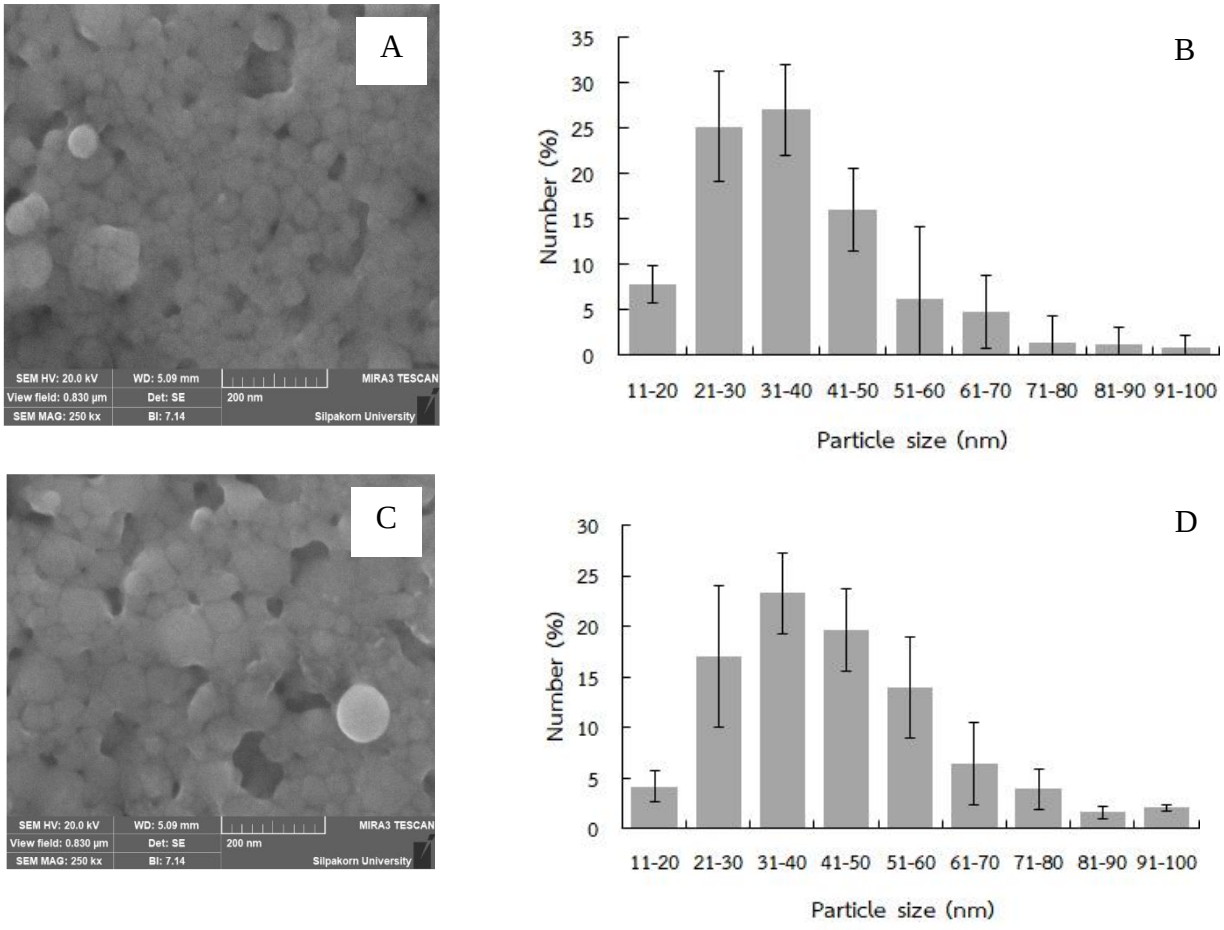

Figure 2 Scanning electron microscopy images and size distribution of SeNP-G4 (at 4 h of incubation, 2A and 2B) and SeNP-G72 (at 72 h of incubation, 2C and 2D)

Nanoparticles with zeta potential between -10 and +10 mV are considered approximately neutral, whereas those with zeta potential greater than +30 mV or less than -30 mV are considered strongly cationic and anionic, respectively. The zeta potential of both SeNPs was negative (-23.8 mV and -24.2 mV) as presented in Figure 3A and 3B, which indicated that the formed NPs were surrounded by negatively charged groups. Additionally, no difference in charge on the coating was observed as incubation time increased from 4 h to 72 h. The zeta potential of SeNP-G in this study was higher than that of used *Aloe vera* leaf extract (-18 mV), as reported by Fardsadegh et al., 2019. This could be related to various reductant and stabilizing agents used.

However, the high value of zeta potential implied that the synthesized SeNP-G had physical colloidal stability. The PDI values of the fabricated SeNP-G4 and SeNP-G72 were 0.146 and 0.180, respectively, which indicated that the SeNP-G was monodispersed.

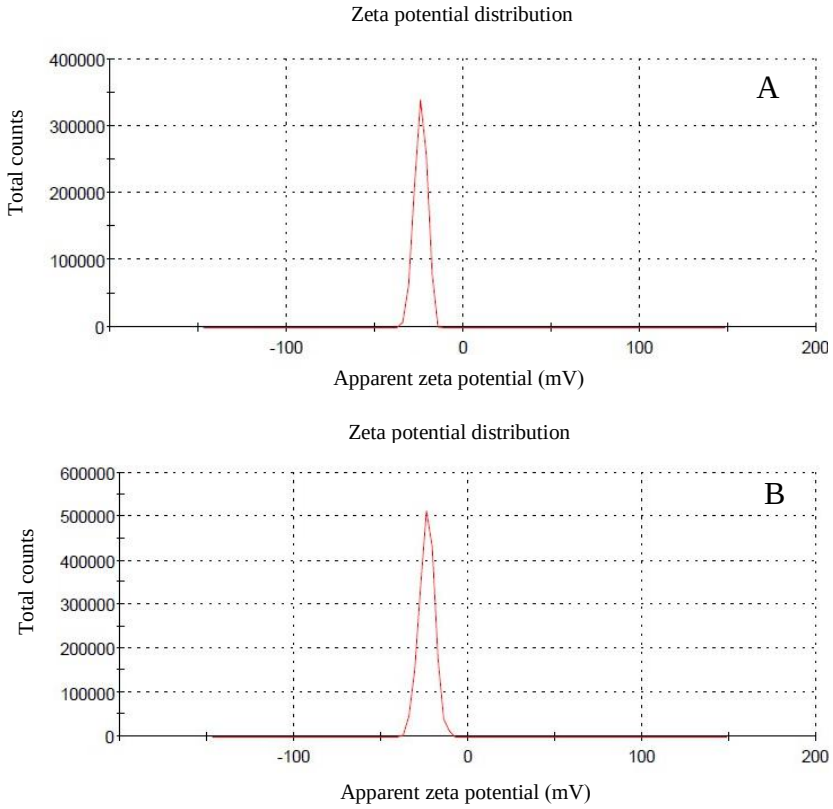

Figure 3 Zeta potential distribution of SeNP-G4 (at 4 h of incubation, 3A) and SeNP-G72 (at 72 h of incubation, 3B)

3.2 Antibacterial properties

3.2.1 Inhibition zones (agar diffusion method)

The selenium nanoparticles, SeNP-G4 and SeNP-G72, had antibacterial activity against *S. aureus,* as shown by a clear zone with average sizes presented in Table 1. This condition revealed that both SeNP-Gs provided a larger clear zone as their concentrations increased while SeNP-G4 seemed to be slightly more potent in antibacterial activity than SeNP-G72. No clear zone around the well with garlic extract concentration at 10 mg/mL was observed. This condition implied that antibacterial activity of SeNP-G could be mainly attributed to sodium selenite. However, fresh garlic extract has been reported to have anti-bacterial property due to its allicin content (Durairaj et al., 2009). The ineffectiveness of the garlic extract used in this study was probably due to either the insufficient content of allicin from garlic extract that diffused to high bacterial concentration (35×10^6 cells) or the development of bacterial biofilm that prevented allicin penetration to affect the cell. Therefore, a more sensitive method of antibacterial assay was performed using bacterial number at $1\text{-}2 \times 10^5$ cells/mL in turbidity test, where samples directly reach the target without the blocking diffusion effect as in the agar diffusion method.

Table 1 Size of bacterial inhibition clear zone after 24 h incubation with tested materials

Sample	Clear zone average size ± SD (mm)
Sodium selenite 10 mM (1.73 mg/mL)	11.58 ± 0.340
SeNP-G4 (5 mg/mL)	12.08 ± 0.630
SeNP-G4 (10 mg/mL)	12.88 ± 0.050
SeNP-G72 (5 mg/mL)	10.11 ± 0.748
SeNP-G72 (10 mg/mL)	11.25 ± 1.580
Garlic (10 mg/mL)	-
Penicillin and streptomycin (100 U)	20.16 ± 0.635

SeNP-G4 = SeNPs at 4 h of incubation

SeNP-G72 = SeNPs at 72 h of incubation

3.2.2 Inhibition turbidity values

SeNP-G4 and SeNP-G72 exhibited antibacterial inhibition against *S. aureus* in a dose-dependent manner by turbidity test (Figure 4 A), whereas no significant difference in bacterial inhibition activity was observed between SeNP- G4 and SeNP- G72. The ability of both SeNP-Gs to inhibit *S. aureus* was approximately 92% at the highest concentration used in the test. Similarly, garlic extract, sodium selenite, penicillin, and streptomycin demonstrated bacterial inhibition activity in relation to the concentration to a certain extent (60%-80%), as shown in Figure 4B, 4C, and 4D. This condition confirmed the antibacterial activity of SeNP-G over sodium selenite and garlic extract. The inhibitory effect of SeNP-G on Gram-positive bacteria of *S. aureus* may be due to the chemisorption of SeNP-G on the cell wall, penetration through peptidoglycan membrane, and entrance to kill the cell (Guisbiers et al., 2016). The size of SeNP-G may play a role in bacterial inhibition because SeNP-G4 showed a slightly higher inhibition activity than the SeNP-G72 at the concentration lower than 50 (µg/mL). The smaller particles can possibly diffuse and attack the bacterial cell wall better than the large particles can. Inside the bacterial cell, SeNPs can also behave as pro-oxidant and cause *S. aureus* cell death through generation of reactive oxygen species due to antibacterial mechanism of metal nanoparticles similar to what has been reported for AgNPs (Qing et al., 2018). A similar extent of *S. aureus* inhibition of sodium selenite and SeNP-G was observed on the size of the clear zone as presented in Table 1. Therefore, cytotoxicity test of the chemicals was performed on normal cells to verify the applicability of SeNP-G as an antibacterial agent used on human skin.

3.2.3 Cytotoxicity test

The cytotoxicity test showed that sodium selenite was toxic to normal fibroblast cells of MRC-5 with IC50 at 2.04 (µg/mL) as shown in Table 2, whereas the SeNP-G4 and SeNP-G72 were less toxic with IC50 at 136.78 (µg/mL) and 219. 78 (µg/mL), respectively. Almost twice lower IC50 of SeNP-G72 than that of SeNP-G4 implied that the SeNP-G72 might be more practical for use. Considering the IC50 from both types of cells, MRC-5 and *S. aureus*, we found that SeNP-G could be a safer antibacterial agent than sodium selenite. From this result, we can infer that the nano-formation with plant extract could reduce the toxicity of sodium selenite and make it more applicable for general use.

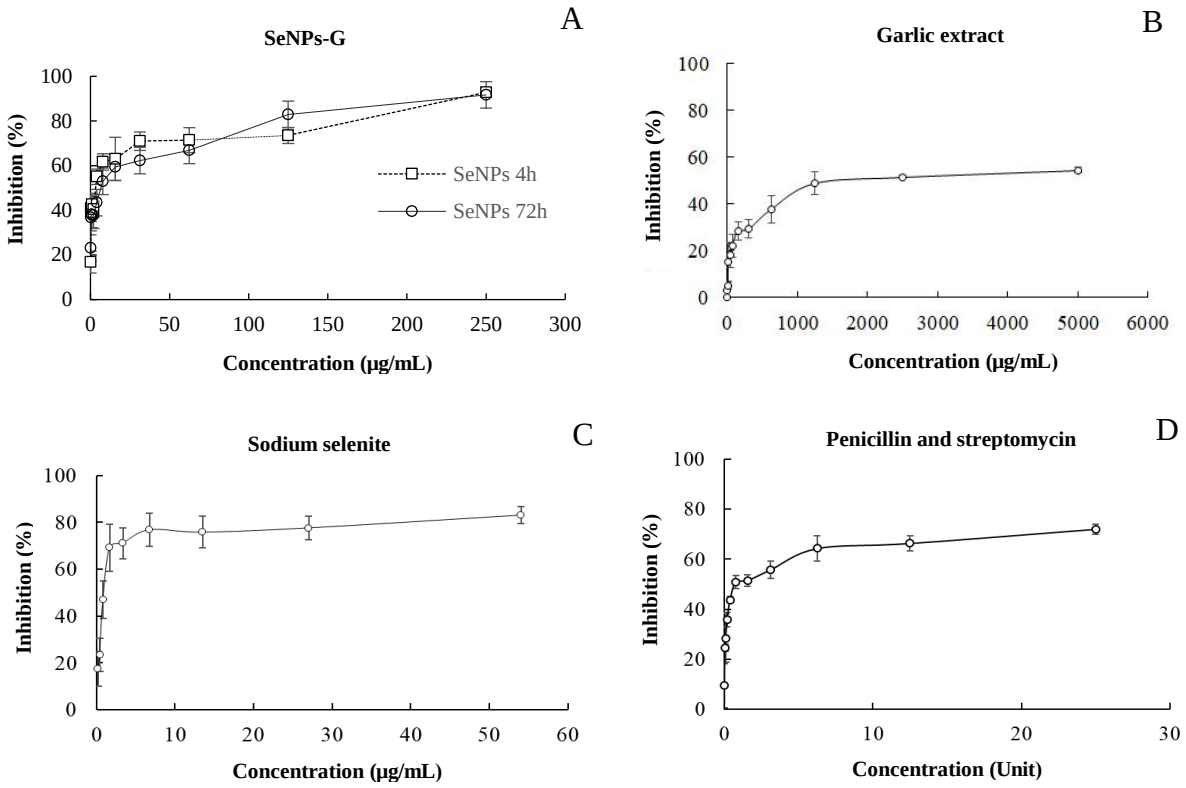

Figure 4 Percentage of bacterial inhibition at various concentrations of SeNP-G4 and SeNP-G72 (A), garlic extract (B), sodium selenite (C), penicillin and streptomycin (D)

Table 2 Inhibition concentration (IC50) of sodium selenite and SeNP-G on MRC-5 cells and *S. aureus*

IC_{50} (µg/mL)	Sodium selenite	SeNP-G4	SeNP-G72
S. aureus	$1.90^{a} \pm 0.25$	$5.34^{a} \pm 0.68$	$3.5^{b} \pm 0.35$
MRC-5	$2.04^{a} \pm 0.85$	$136.78^{b} \pm 25.88$	$219.78^{c} \pm 20.03$

[a, b, c] Each value had a significant difference ($P < 0.05$) within each row

4. CONCLUSION

The specific nanoselenium character of SeNP-G4 and SeNP-G72 was presented as the red brick solution with maximum absorbance at 270-280 nm. The particles were spherical in shape with size range in nanometer as determined by SEM. Longer curing time resulted in a slightly larger particle size of SeNP-G72 (41-50 nm) compared with SeNP-G4 (21-40 nm). However, the particles were monodispersed and had physical colloidal stability. No marked difference in bacterial inhibition activity was observed between SeNP-G4 and SeNP-G72 with different particle sizes. However, the antibacterial activity was mainly derived from sodium selenite rather than garlic extract. SeNP-G was a more applicable antibacterial agent because it was safer than sodium selenite.

ACKNOWLEDGMENT

We are grateful to Mrs. Surat Punyahathaikul from the Institute of Molecular Biosciences at Mahidol

University for her assistance in this project. We also thank the Department of Biotechnology, Faculty of Engineering and Industrial Technology at Silpakorn University, where our research work was conducted. We acknowledge the financial support provided by the Agricultural Research Development Agency (Grant No. CRP6105021330).

REFERENCES

Anu, K., Singaravelu, G., Murugan, K., and Benelli, G. (2017). Green-synthesis of selenium nanoparticles using garlic cloves (*Allium sativum*): Biophysical characterization and cytotoxicity on vero cells. *Journal of Cluster Science*, 28 (1), 551-563.

Durairaj, C., Kim, S. J., Edelhauser, H. F., Shah, J. C., and Kompella, U. B. (2009). Influence of dosage form on the intravitreal pharmacokinetics of diclofenac. *Investigative Ophthalmology & Visual Science*, 50(10), 4887- 4897.

Ezhuthupurakkal, P. B., Polaki, L. R., Suyavaran, A., Subastri, A, Sujatha, V., and Thirunavukkarasu, C. (2017). Selenium nanoparticles synthesized in aqueous extract of *Allium sativum* perturbs the structural integrity of calf thymus DNA through intercalation and groove binding. *Materials Science and Engineering*, 74(1), 597-608.

Fardsadegh, B., Vaghari, H., Mohammad-Jafari, R., Najian, Y., and Jafarizadeh-Malmiri, H. (2019). Biosynthesis, characterization and antimicrobial activities assessment of fabricated selenium nanoparticles using *Pelargonium zonale* leaf extract. *Green Processing and Synthesis*, 8(1), 191-198.

Fujisawa, H., Suma, K., Origuchi, K., Kumagai, H., Seki, T., and Ariga, T. (2008). Biological and chemical stability of garlic-derived allicin. *Journal of Agricultural and Food Chemistry*, 56(11), 4229-4235.

Guisbiers, G., Wang, Q., Khachatryan, E., Mimun, L. C., Mendoza-Cruz, R., Larese-Casanova, P., Webster, T. J., and Nash, K. L. (2016). Inhibition of *E. coli* and *S. aureus* with selenium nanoparticles synthesized by pulsed laser ablation in deionized water. *International Journal of Nanomedicine*, 11, 3731-3736.

Hosnedlova, B., Kepinska, M., Skalickova, S., Fernandez, C., Ruttkay-Nedecky, B., Peng, Q., Baron, M., Melcova, M., Opatrilova, R., Zidkova, J., Bjorklund, G., Sochor, J., and Kizek, R. (2018). Nano-selenium and its nanomedicine applications: a critical review. *International Journal of Nanomedicine*, 13, 2107-2128.

Khiralla, G. M., and El-Deeb, B. A. (2015). Antimicrobial and antibiofilm effects of selenium nanoparticles on some foodborne pathogens. *LWT - Food Science and Technology*, 63(2), 1001-1007.

Lin, Z. H., and Chris Wang, C. R. (2005). Evidence on the size-dependent absorption spectral evolution of selenium nanoparticles. *Materials Chemistry and Physics*, 92(2-3), 591-594.

Menon, S., Shrudhi Devi, K. S., Santhiya, R., Rajeshkumar, S., and Venkat Kumar, S. (2018). Selenium nanoparticles: A potent chemotherapeutic agent and an elucidation of its mechanism. *Colloids and Surfaces B: Biointerfaces*, 170, 280-292.

Mittal, A. K., Chisti, Y., and Banerjee, U. C. (2013). Synthesis of metallic nanoparticles using plant extracts. *Biotechnology Advances*, 31(2), 346-356.

Nguyen, T. H. D., Vardhanabhuti, B., Lin, M., and Mustapha, A. (2017). Antibacterial properties of selenium nanoparticles and their toxicity to Caco-2 cells. *Food Control*, 77, 17-24.

Qing, Y., Cheng, L., Li, R., Liu, G., Zhang, Y., Tang, X., Wang, J., Liu, H., and Qin, Y. (2018). Potential antibacterial mechanism of silver nanoparticles and the optimization of orthopedic implants by advanced modification technologies. *International Journal of Nanomedicine*, 13, 3311-3327.

Ramamurthy, C., Sampath, K. S., Arunkumar, P., Suresh Kumar, M., Sujatha, V., Premkumar, K., and Thirunavukkarasu, C. (2013). Green synthesis and characterization of selenium nanoparticles and its augmented cytotoxicity with doxorubicin on cancer cells. *Bioprocess and Biosystems Engineering*, 36(8), 1131-1139.

Ratthawongjirakul, P., and Thongkerd, V. (2016). Fresh garlic extract inhibits *Staphylococcus aureus* biofilm formation under chemopreventive and chemotherapeutic conditions. *Songklanakarin Journal of Science and Technology*, 38(4), 381-389.

Sharma, G., Sharma, A. R., Bhavesh, R., Park, J., Ganbold, B., Nam, J. S., and Lee, S. S. (2014). Biomolecule-mediated synthesis of selenium nanoparticles using dried *Vitis vinifera* (raisin) extract. *Molecules*, 19(3), 2761-2770.

Skov, R. L., and Jensen, K. S. (2009). Community-associated meticillin-resistant *Staphylococcus aureus* as a cause of hospital-acquired infections. *Journal of Hospital Infection*, 73(4), 364-370.

Tran, P. A., and Webster, T. J. (2011). Selenium nanoparticles inhibit *Staphylococcus aureus* growth. *International Journal of Nanomedicine*, 6, 1553-1558.

Vyas, J., and Rana, S. (2017). Antioxidant activity and green synthesis of selenium nanoparticles using *allium sativum* extract. *International Journal of Phytomedicine*, 9(4), 634-641.

Wang, J. C. , Neogi, P., and Forciniti, D. (2006). On one-dimensional self-assembly of surfactant-coated nanoparticles. *The Journal of Chemical Physics*, 125(19), 194717.

Zhang, J., Gao, X. Y., Zhang, L. D., and Bao, Y. P. (2001). Biological effects of a nano red elemental selenium. *Biofactors*, 15(1), 27-38.